

## Neutrality of Taper-Ended Tubular Grains

{H. R. Noaman, M. Y. Ahmed\*, H. M. Abdalla and M. A. Al-Sanabawy}†

**Abstract:** In many applications, a constant thrust of the solid propellant rocket motor (SPRM) throughout the operating time is desired. Such thrust-time scenario is known as neutral burning. Typically, tubular grains with internal burning surface yield a progressive thrust-time history and, therefore, if a neutral thrust-time history is required, the progression in the burning surface should be compensated by including the side faces as well.

However, neutrality of tubular grain that burns at both of the internal and end surfaces is subject to a limited range of slenderness ratio. Tapering the port at the end faces of the tubular grain would expand the range of the slenderness ratio that ensures neutrality. In the present paper, the issue of neutrality of taper-ended tubular grain is explored. For the studied case, it was found that with normal-ended tube grains neutrality can be realized for slenderness ratio 1.8 and web-to-radius ratio 0.4. However, keeping the same web-to-radius ratio and tapering the ends at angle 25° would slightly worsen the volumetric filling coefficient (~ 15% less), but burning neutrality could be attained for slenderness ratios as high as 2.54 (~ 40% higher).

With this practice, it is possible to maintain neutrality where much longer grains may be adopted for certain applications.

**Keywords:** Neutral burning, taper-ended tubular grain, solid propellant grain, solid propellant rocket motor.

### Nomenclature

$A_b$	Burning area
$A_b^*$	Burning area divided by grain outer diameter area
$D_{in}$	Inner diameter of propellant grain
$D_{out}$	Outer diameter of propellant grain
$K_{fc}$	Volumetric filling coefficient
$L$	Length of grain
$L_{out}$	outer length of the grain
$L_{in}$	Length of inner straight part of the grain
$L^*$	Length-to-diameter ratio
$y$	Instantaneous burnt distance
$\theta$	Tapering angle
$\tau^*$	Twice web thickness divided by outer diameter of grain.
$\tau$	Web thickness

\* Egyptian Armed Forces, Egypt, [mym141101@yahoo.com](mailto:mym141101@yahoo.com).

† Egyptian Armed Forces, Egypt.

## 1. Introduction

Thrust magnitude control (or thrust modulation) is one of potential requirements addressed in some rocket applications. While this is a relatively practicable task in case of liquid propellant rocket motors where the propellant flow can be modified during flight, it is unmanageable to modify the thrust of a solid propellant rocket motor (SPRM) once ignited. The SPRM designers have to answer the opposite question: “for a required course of thrust, what should be the design measures to achieve such course of thrust?”. During the design phase a process of tailoring some parameters would permit a reasonable predictable thrust history. Grain geometry, inhibition of some surfaces, use of more than one propellant composition are some parameters to address for thrust tailoring. With a clever deliberate design, when the rocket is fired, its thrust should follow the predicted course within a specified envelope.

The thrust program can be progressive, regressive, neutral, or assume any other pattern for a given propellant, Fig. 1. In progressive thrust, the burning surface area increases with time whereas in the regressive thrust program, the burning surface area decreases with time. In the neutral thrust program, the burning surface area, and hence, pressure and thrust remain approximately constant, typically within about  $\pm 15\%$ .

In the present treatment the burning neutrality is defined as the ratio of the maximum burning surface to the average burning surface encountered during the burning duration. In such a way it would be convenient to consider a mathematical expression as an estimate of neutrality to be used for further analysis.

Burning neutrality is strongly required with guided missile where a nearly constant thrust is necessary for proper control. Some trade-off studies may require geometric adaptations concurrent with neutrality. In this context, the slenderness ratio, the filling coefficient, tapering ends will be discussed in view of burning neutrality.

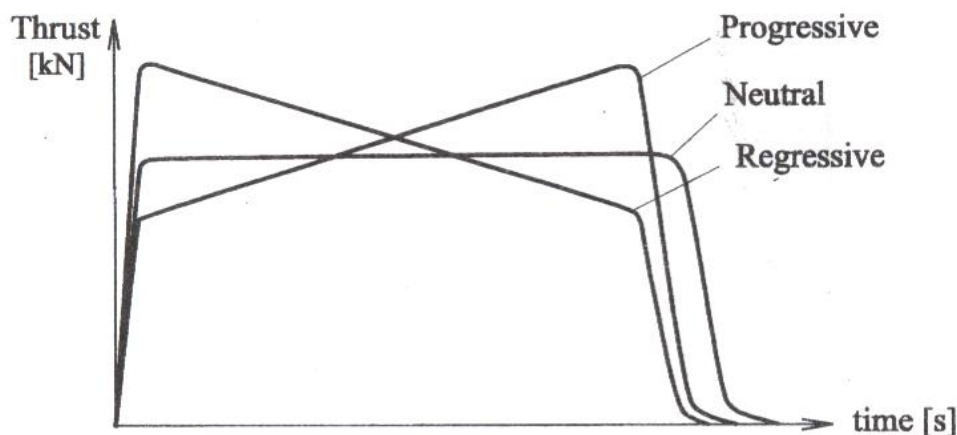


**Fig. 1. Typical thrust-time programs**

In the majority of cases the thrust of the rocket is required to be constant during the whole time of function. One of the well-known grain configurations that yield neutral burning is the typical tubular grain in which the grain is burnt from both of the inner and end faces, Fig. 2.

The geometry of this grain is defined by the outer diameter  $D_{out}$ , the inner diameter  $D_{in}$ , the grain length  $L$  and the web thickness  $\tau$ .

The objective of the present study is to discuss the neutrality of these tubular grains, and to which extent a tapering at the ends would improve neutrality.

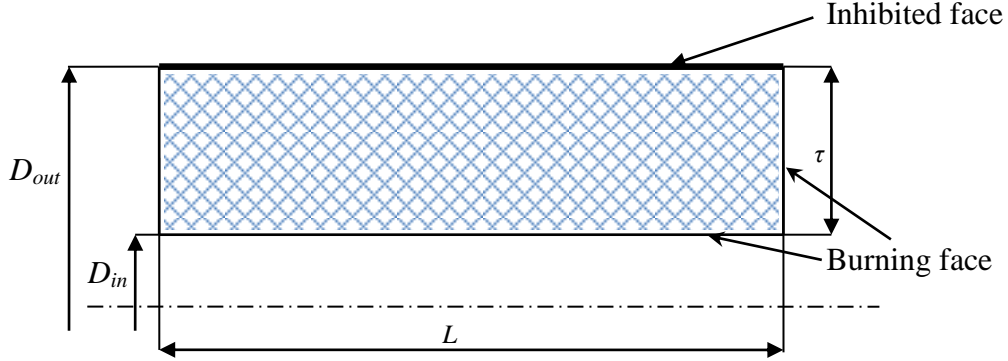


**Fig. 2. Geometry of tubular grain**

Neutrality of such grain design is not always guaranteed. The dependence of neutrality on the values of  $(L/D_{out})$  and  $(\tau/D_{out})$  will be investigated in this paper.

## 2. Mathematical Model

The geometry of a taper-ended tubular grain is illustrated in Fig. 3. Notice that only the outer face is inhibited. Here  $H$ ,  $\theta$  and  $L_{in}$  present the tapering length, the tapering angle and the length left without tapering. During the burning process, the burning surface moves parallel to the initial surface. At any instant of time, the dashed line marks the instantaneous burning surface.

For a given  $y$  the burning area can be expressed as

$$A_b = \pi(D_{in} + 2y)(L - H - 2y \tan \frac{\theta}{2}) + \frac{2\pi}{2}(D_{in} + 2y + D_{out}) \frac{1}{\cos \theta} (H - \frac{y}{\tan \theta}) \quad (1)$$

where:

$$L = \frac{L_{out} + L_{in}}{2} \quad (2)$$

$$H = \tau / \tan \theta \quad (3)$$

From trigonometric relations

$$\tan \frac{\theta}{2} = \frac{1}{\sin \theta} - \frac{1}{\tan \theta} \quad (4)$$

From Eqs. 1 – 4 one gets



$$\tau^* = 2 \cdot \tau / D_{out} \quad (7)$$

$$y^* = y / \tau \quad (8)$$

$$L^* = L / D_{out} \quad (9)$$

From Eqs. 6 - 9 one gets

$$A_b^* = 4L^* + \frac{4\tau^*}{\sin \theta} - \frac{2\tau^*}{\tan \theta} - \frac{8y^* \tau^*}{\sin \theta} + \frac{4y^* \tau^*}{\tan \theta} - 4\tau^* L^* + 4y^* L^* \tau^* + \frac{2\tau^{*2}}{\tan \theta} - \frac{2\tau^{*2}}{\sin \theta} + \frac{8\tau^{*2} y^*}{\sin \theta} - \frac{6y^* \tau^{*2}}{\tan \theta} - \frac{6y^{*2} \tau^{*2}}{\sin \theta} + \frac{4y^{*2} \tau^{*2}}{\tan \theta} \quad (10)$$

This equation can be rewritten in a more compact form as:

$$A_b^* = a + by^* + cy^{*2} \quad (11)$$

where:

$$a = 4L^* + \frac{4\tau^*}{\sin \theta} - \frac{2\tau^*}{\tan \theta} - 4\tau^* L^* + \frac{2\tau^{*2}}{\tan \theta} - \frac{2\tau^{*2}}{\sin \theta} \quad (12)$$

$$b = -\frac{8y^* \tau^*}{\sin \theta} + \frac{4y^* \tau^*}{\tan \theta} - 4\tau^* L^* + 4y^* L^* \tau^* + \frac{8\tau^{*2} y^*}{\sin \theta} - \frac{6y^* \tau^{*2}}{\tan \theta} \quad (13)$$

$$c = -\frac{6y^{*2} \tau^{*2}}{\sin \theta} + \frac{4y^{*2} \tau^{*2}}{\tan \theta} \quad (14)$$

Following the proposed definition of the burning neutrality given by the ratio of the maximum burning surface to the average burning surface encountered during the burning duration:

$$N_r = A_{b \max}^* / A_{b \text{ av}}^* \quad (15)$$

where

$$A_{b \max}^* = a - b^2 / 4c \quad (16)$$

$$A_{b \text{ av}}^* = a + b/2 + c/3 \quad (17)$$

### 3. Results and Discussion

It is evident from the previous section that the burning area is a function of the grain length, the tapering angle, the web thickness and the burnt distance. Considering the dimensionless arguments it holds:  $A_b^* = fn(L^*, \theta, \tau^*, y^*)$ .

#### 3.1 Variation of burning area with the burnt distance

The Figs. 4-6 illustrate the course of variation of the burning area  $A_b^*$  as the burnt distance  $y^*$  increases from 0 to 1 where  $\tau^*=0.4$  for different values of  $L^*$  and  $\theta$ . The figures are plotted for the values of  $\theta = 90^\circ, 45^\circ, \text{ and } 25^\circ$  to examine the burning neutrality in these cases. Table 1 summarizes the cases of progressive, regressive and neutral burning as realized from these figures.

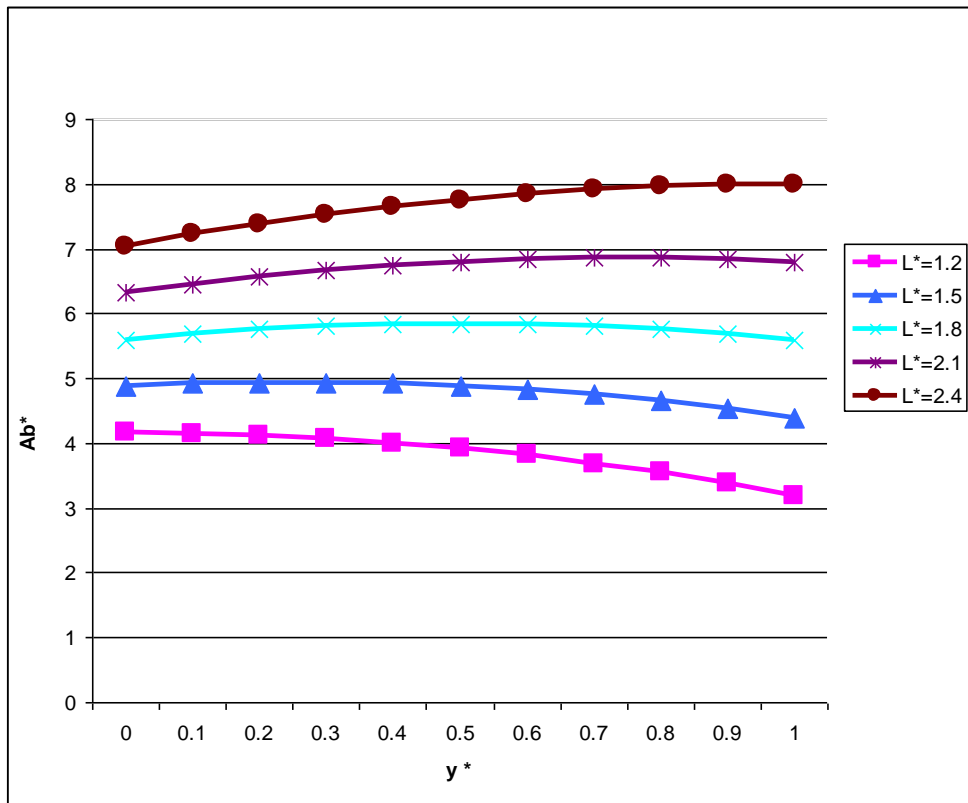


Fig. 4 The burning area  $A_b^*$  versus  $y^*$  for different  $L^*$ , ( $\theta=90^\circ, \tau^*=0.4$ )

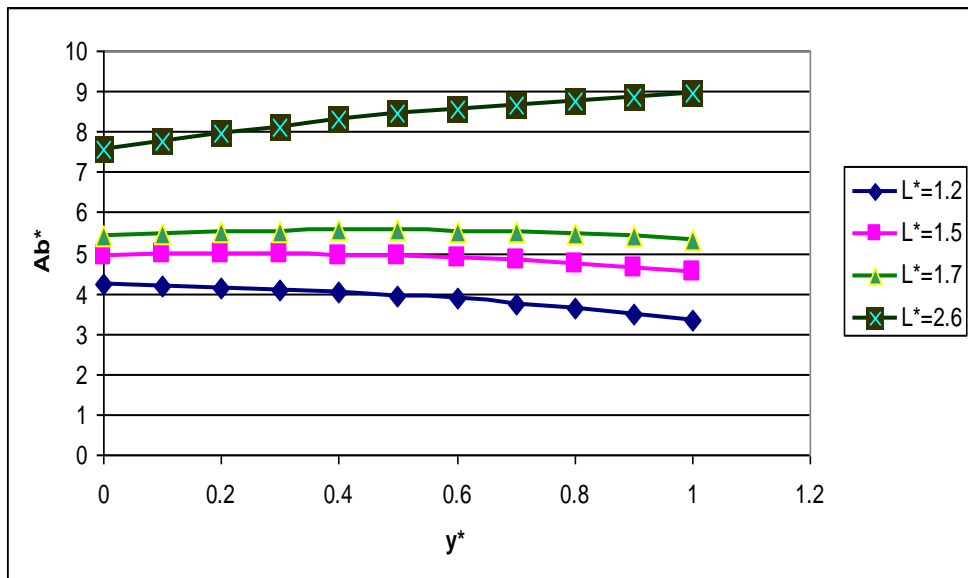


Fig. 5 The burning area  $A_b^*$  versus  $y^*$  for different  $L^*$ , ( $\theta=45^\circ, \tau^*=0.4$ )

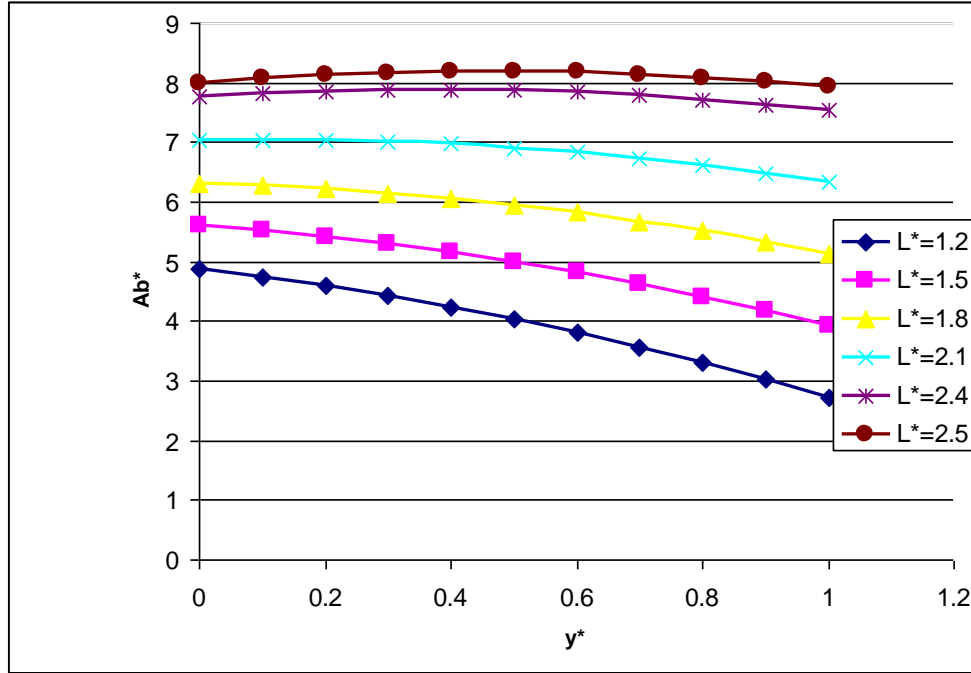


Fig. 6 The burning area  $A_b^*$  versus  $y^*$  for different  $L^*$ , ( $\theta=25^\circ$ ,  $\tau^*=0.4$ )

Table 1 Burning Type at different  $L^*$

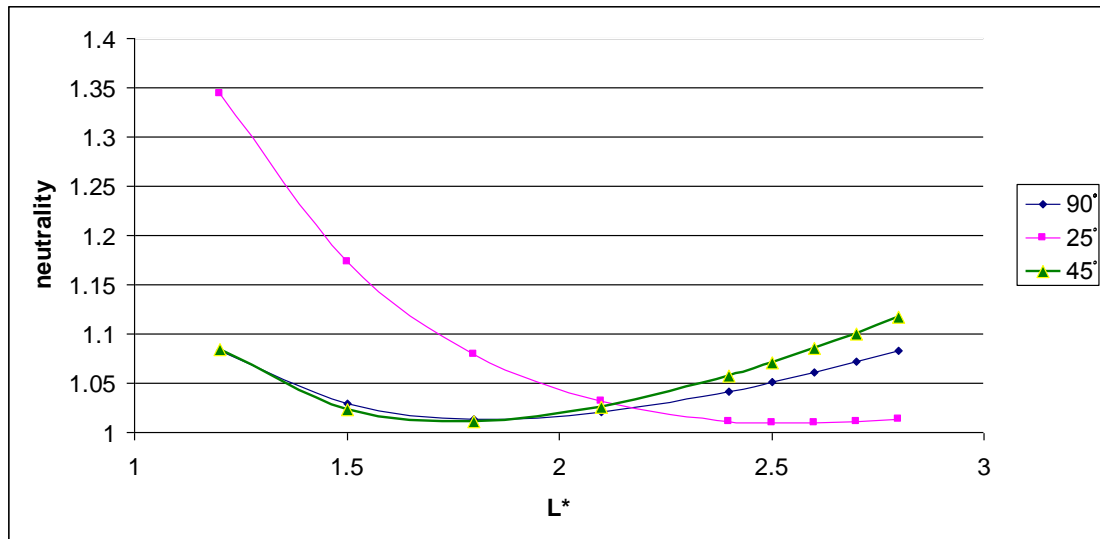
$\theta$	$L^*$	Burning Type
$90^\circ$	1.2	regressive
	1.8	nearly neutral
	2.4	progressive
$45^\circ$	1.2	regressive
	1.7	neutral
	2.6	progressive
$25^\circ$	1.2	regressive
	2.5	neutral

### 3.2 Dependence of Neutrality on the Grain Design

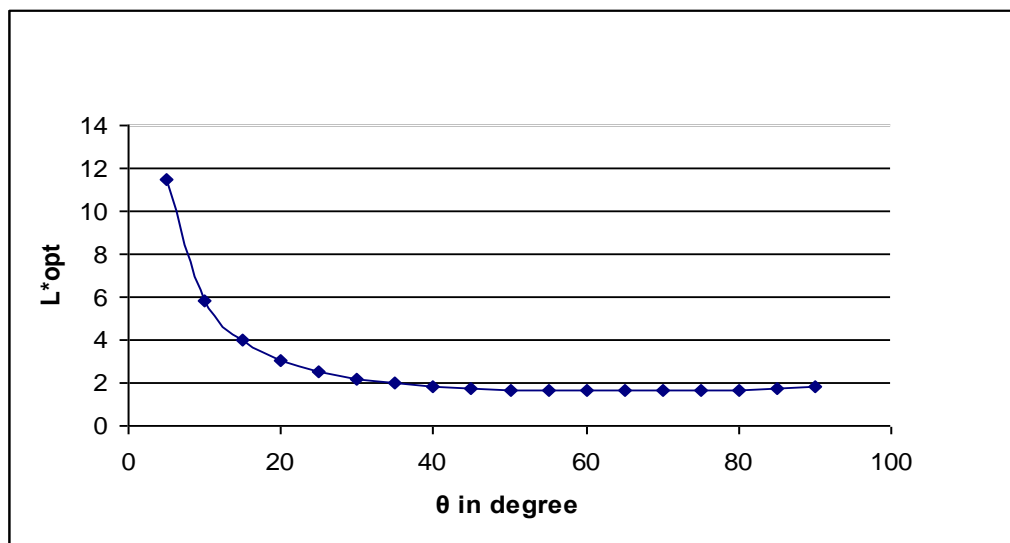
Neutrality can be calculated for different  $L^*$  and  $\theta$ . Figure 9 below shows the neutrality of the grain versus  $L^*$  at  $\tau^*=0.4$  for 3 different tapering angles, namely  $25^\circ$ ,  $45^\circ$  and  $90^\circ$  (no tapering).

Figure 7 demonstrates the dependence of burning neutrality on the grain length  $L^*$  for different tapering angles. The optimum length is the length that corresponds to the best neutrality which is the neutrality more close to 1. As shown, for  $\theta=90^\circ$  (the ends of the grain are non-tapered), the optimum  $L^*$  for neutral burning is 1.8. On the other hand for  $\theta=45^\circ$  and  $\theta=25^\circ$  the optimum  $L^*$  for neutral burning is 1.74 and 2.54 respectively.

It may be concluded that the tapering angle  $\theta$  is a governing factor for reaching neutrality. Figure 8 shows the optimum  $L^*$  tended to achieve neutral burning corresponding to different  $\theta$  at  $\tau^*=0.4$ .



**Fig. 7** Neutrality versus  $L^*$  for different tapering angles  $\theta$  ( $\tau^*=0.4$ )



**Fig. 8**  $L^*_{opt}$  versus tapering angle  $\theta$  ( $\tau^*=0.4$ )

It is clear from Fig. 8 that if neutral burning is required, longer grains (higher  $L^*$ ) imply decreasing the tapering angle  $\theta$ . However decreasing  $\theta$  would increase the free volume and hence worsen the filling coefficient. Figure 9 illustrates the variation of the filling coefficient corresponding to tapering angle. From Figs. 8, 9 it can be shown that as the tapering angle decreases, the filling coefficient of the motor decreases, but  $L^*_{opt}$  increases and vice versa.

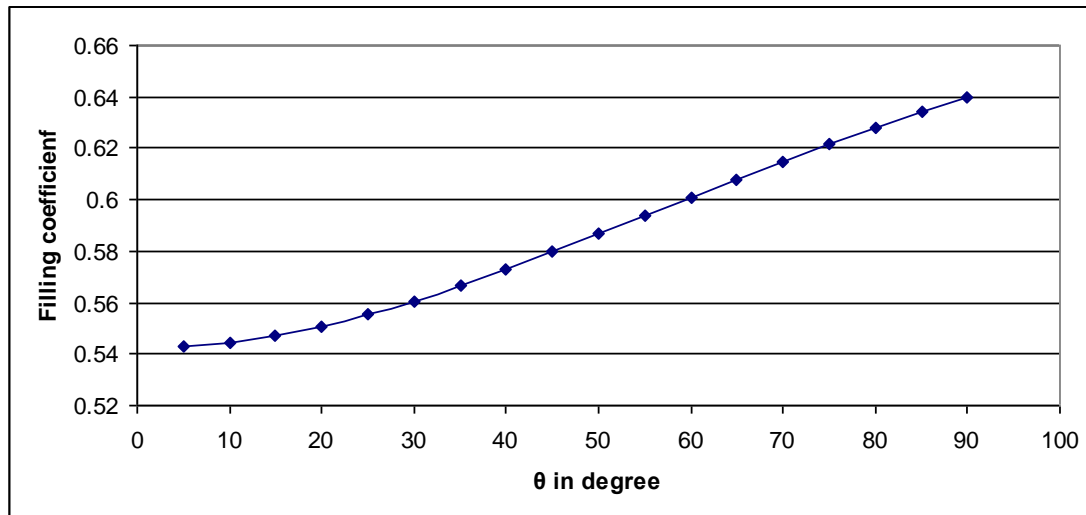


**Fig. 9** Filling coefficient versus tapering angle  $\theta$  ( $\tau^*=0.4, L_{opt}^*$ )

#### 4. Conclusion

Motivated by the requirements imposed by certain applications, neutrality of taper-ended tubular grains was theoretically investigated. It was shown that, neutrality can be realized for slenderness ratio 1.8 for non-taper-ended grains and web-to-diameter ratio 0.4. However, with tapering the ends at angle  $25^\circ$ , and the same web-to-diameter ratio 0.4 the neutrality could be reached with higher slenderness ratio 2.54, while the filling coefficient is degraded.

The developed algorithm allows for examination of the favorable taper-ended grain geometries that optimally satisfies both neutrality and reasonable filling coefficient. The geometric parameters subject to analysis includes web thickness, tapering angles and slenderness ratios.

#### References

- [1] George .P. Sutton, "Rocket Propulsion Element," seventh edition, John Wiley, 1992.
- [2] Barrerre, M., Jaumotte, A., De veubeke, BF. and Vandekerckhove, J., "Rocket Propulsion," Elsevier Publishing Company, 1960.
- [3] G. Püskülcü a and A. Ulas, "3-D Grain Burnback Analysis of Solid Propellant Rocket Motors : Part 2 – Modeling and Simulations", Aerospace Science and Technology, Vol. 12, 2008.
- [4] Halûk aksel, M. and Yildirim, C., "Numerical Simulation of the Grain Burnback in Solid Propellant Rocket Motor" AIAA Paper 2005-4160, 2005.